Supporting Information (SI)

Modulation of the selectivity in anions recognition processes by complexing hydrogen- and halogen- bonding interactions

Fabiola Zapata, Sergio J. Benítez-Benítez, Paula Sabater, Antonio Caballero,* and Pedro Molina *

Departamento de Química Orgánica. Facultad de Química. Universidad de Murcia. Campus de Espinardo, E-30100 Murcia, Spain.

E-mail: ***pmolina@um.es***; ***antocaba@um.es***

Table of contents

Compound 2

^{1}H-NMR ($CDCl_3$, 400 MHz)

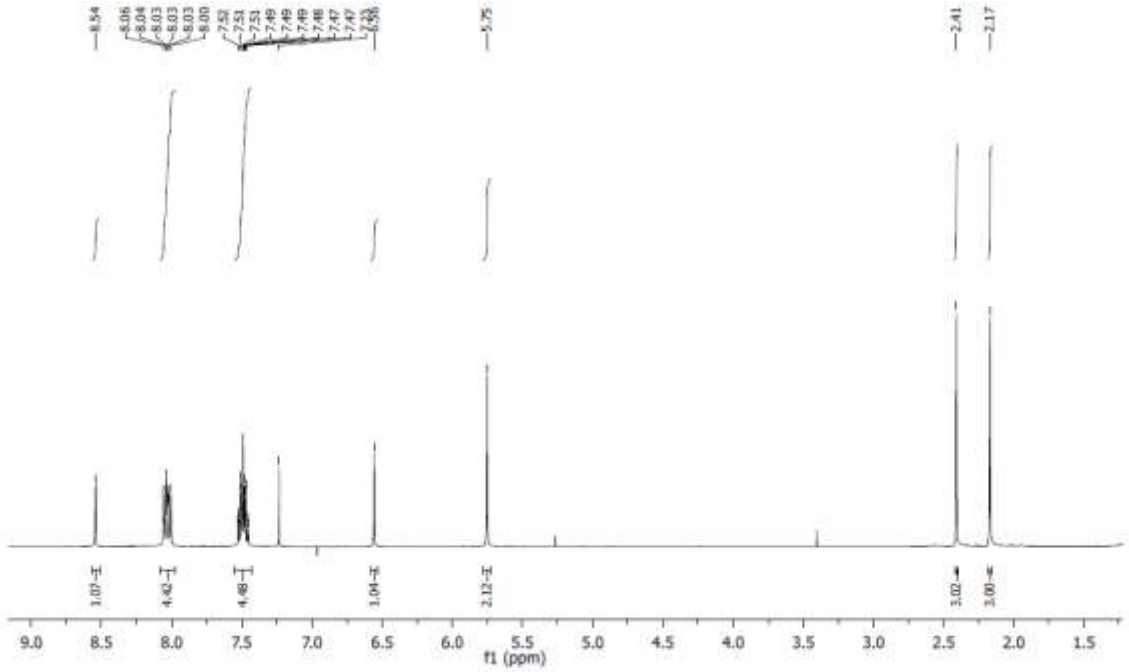

^{13}C NMR (100 MHz, $CDCl_3$)

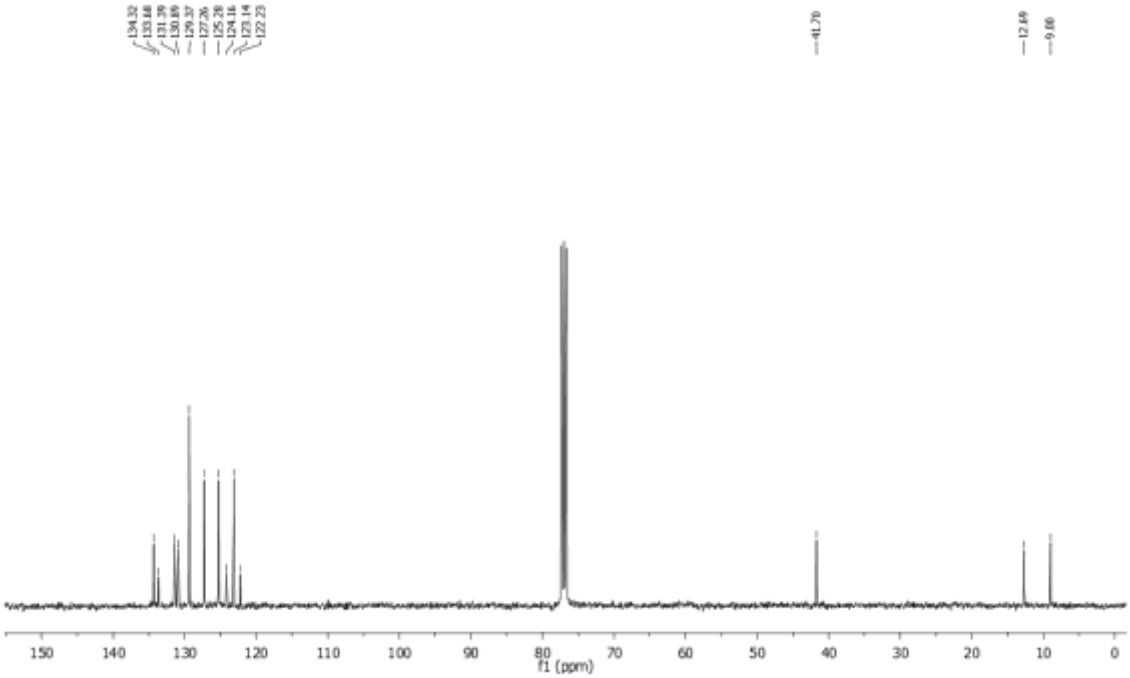

Compound $3^{+}\cdot Br^{-}$

^{1}H-NMR ($CDCl_3$, 400 MHz)

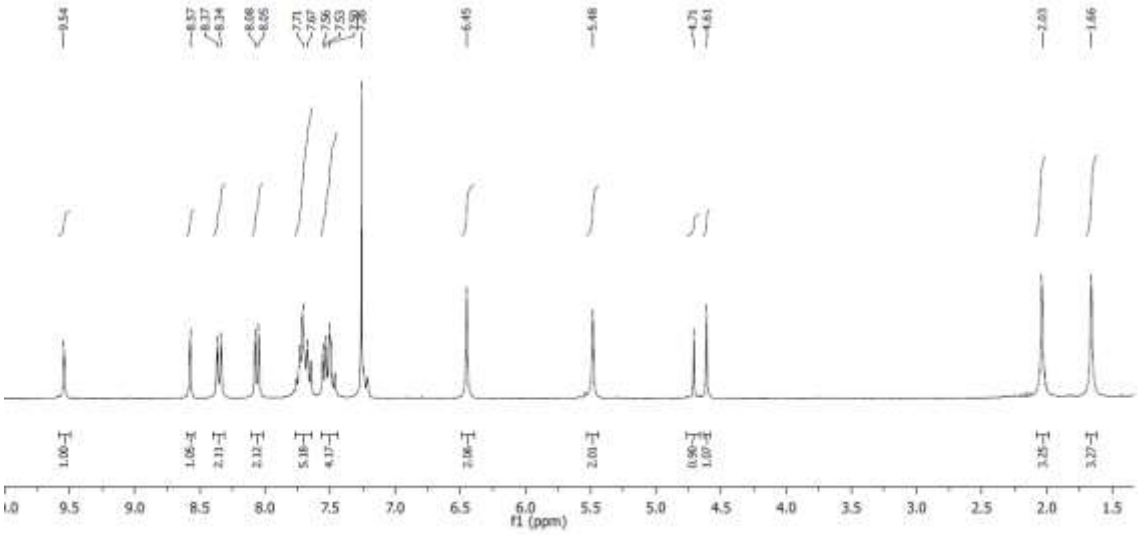

^{13}C-NMR ($CDCl_3$, 75 MHz)

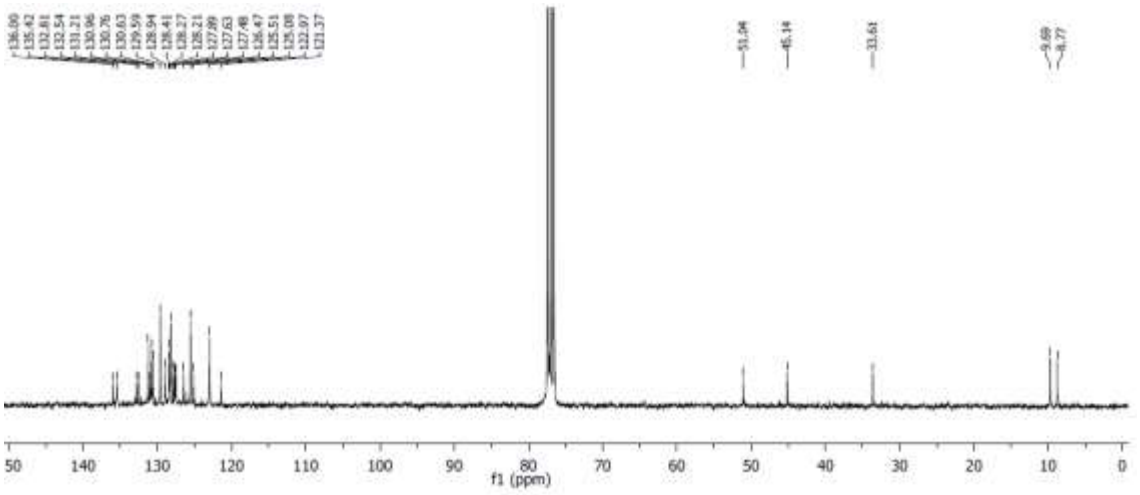

Compound 4

^{1}H-NMR ($CDCl_3$, 400 MHz)

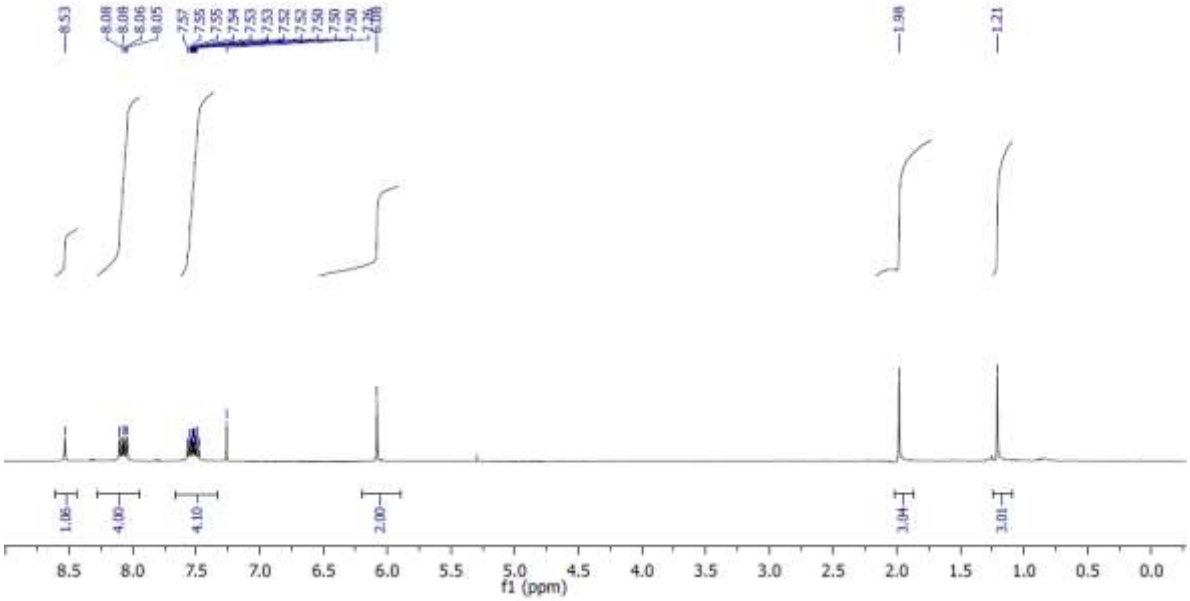

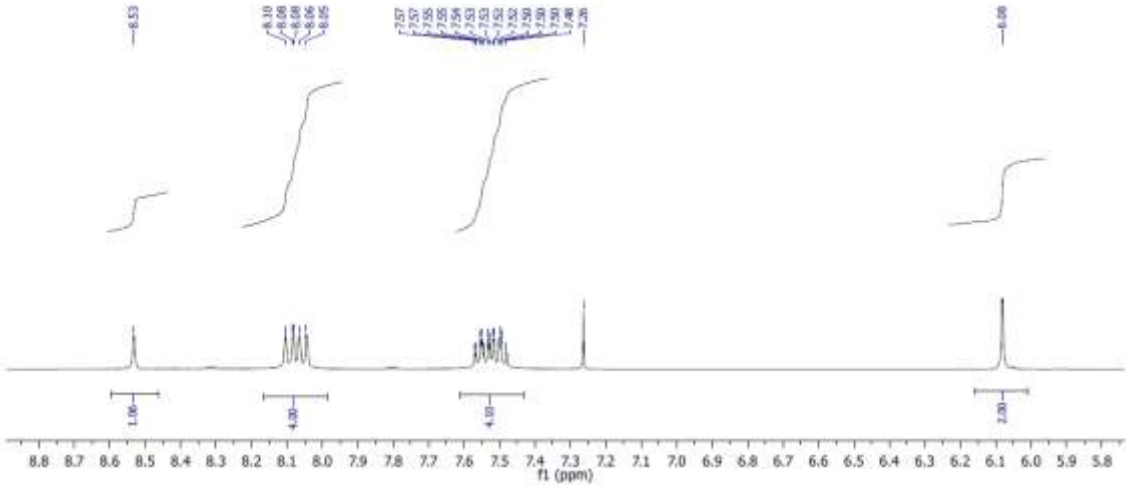

^{13}C-NMR ($CDCl_3$, 100 MHz)

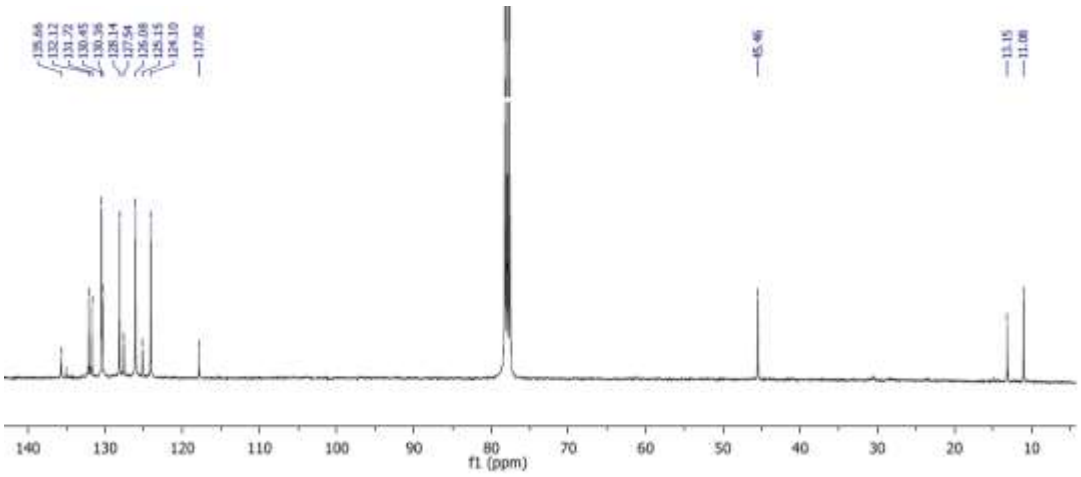

Compound $5^{2+}\cdot 2Br^{-}$

^{1}H-NMR (DMSO, 400 MHz)

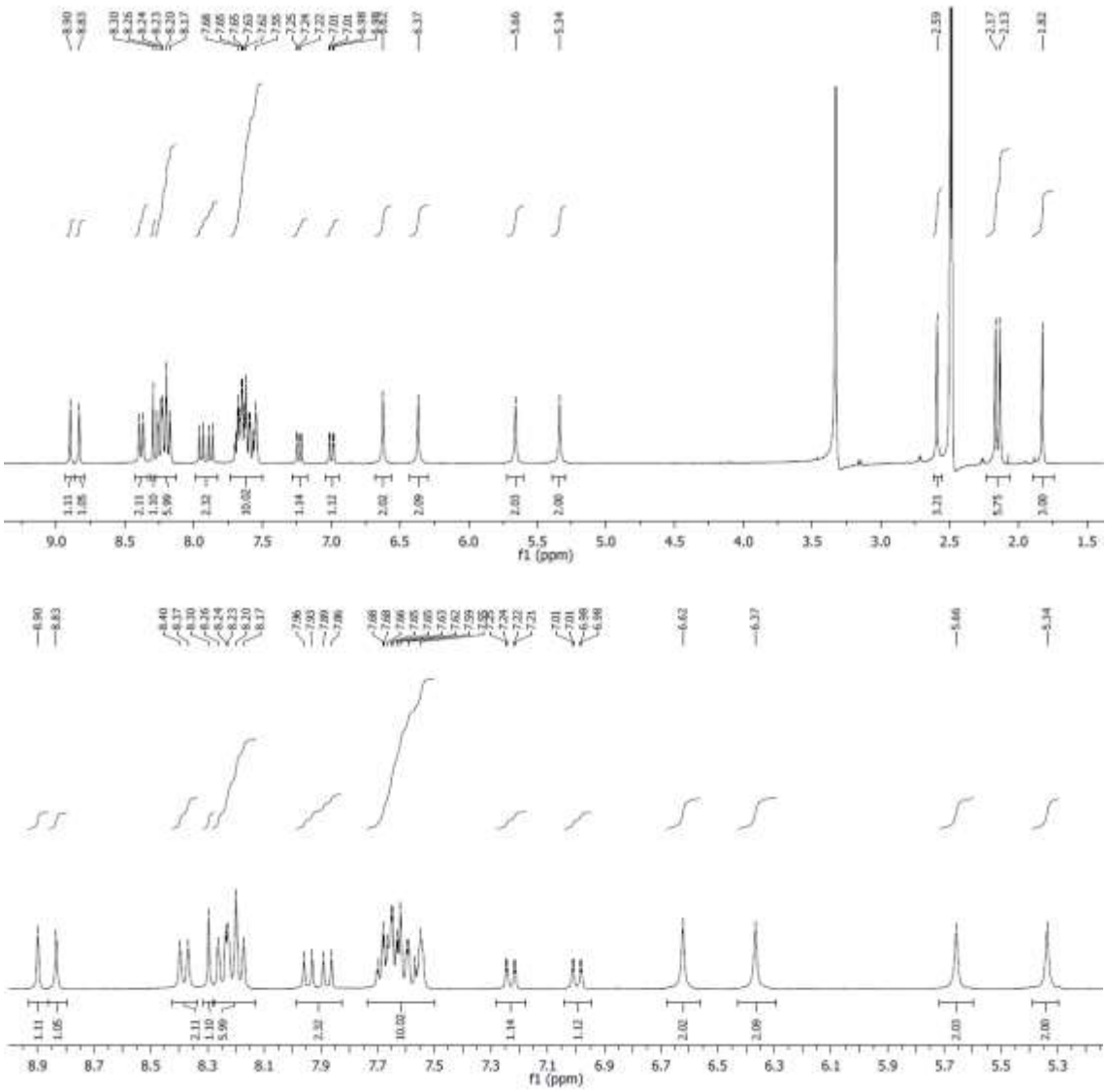

^{13}C-NMR (DMSO, 75 MHz)

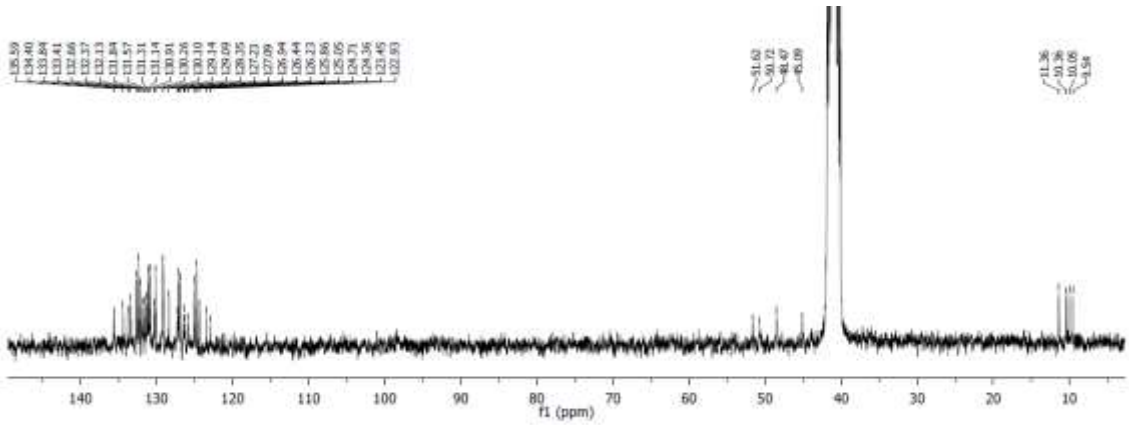

Compound $5^{2+}\cdot 2PF_6^-$

^{1}H-NMR (DMSO, 400 MHz)

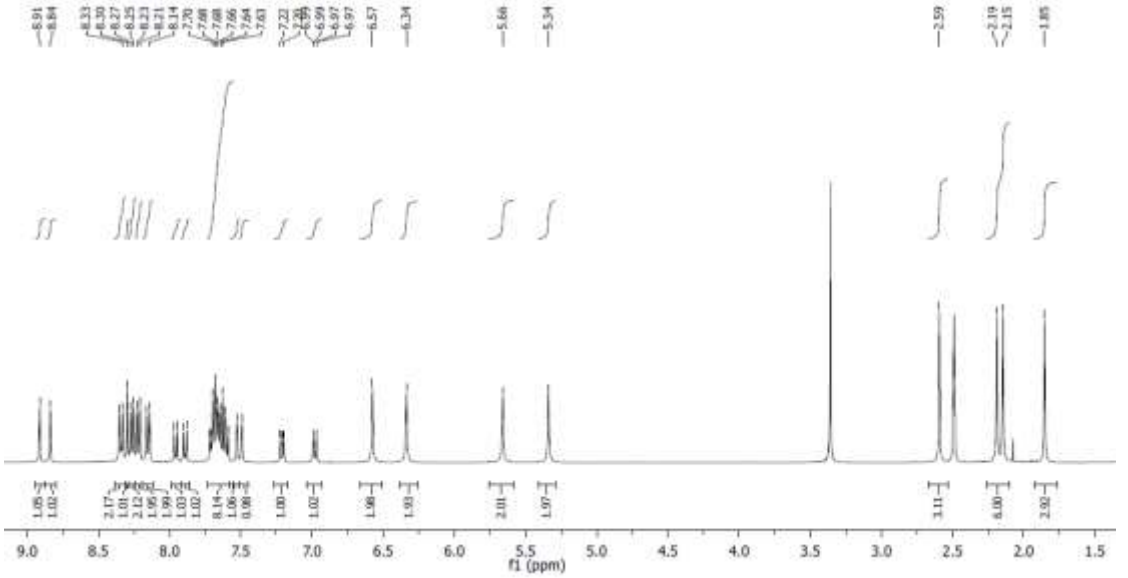

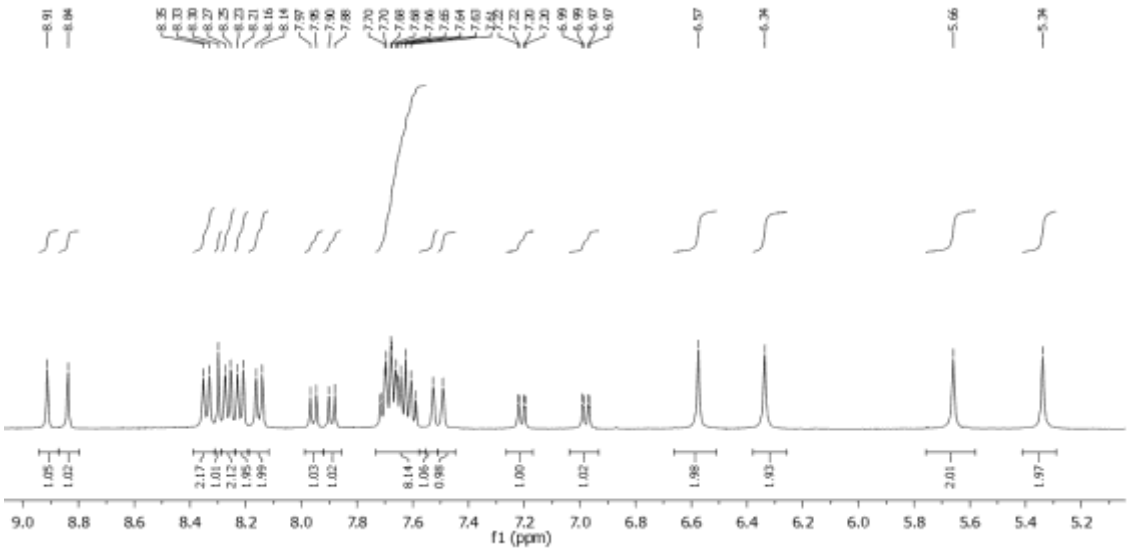

^{13}C-NMR (DMSO, 100 MHz)

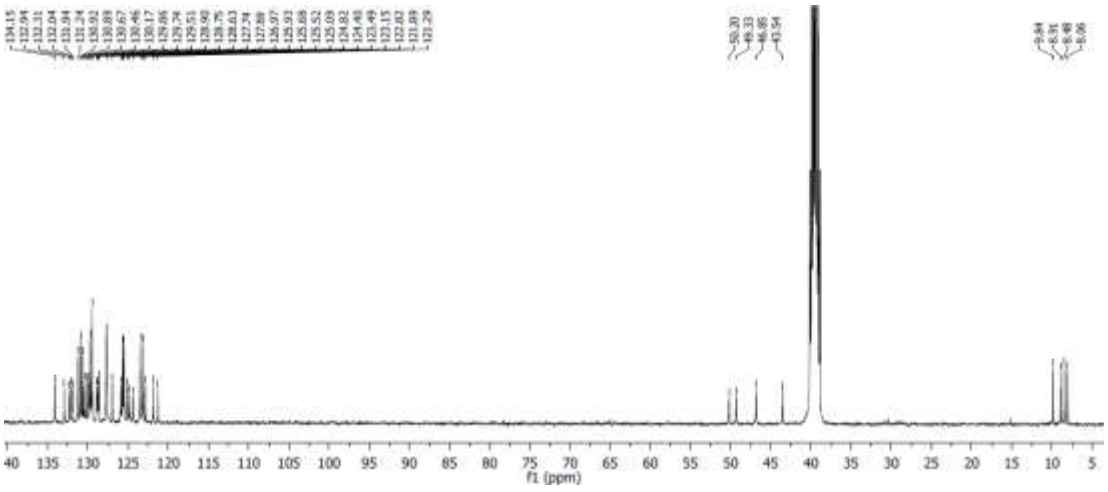

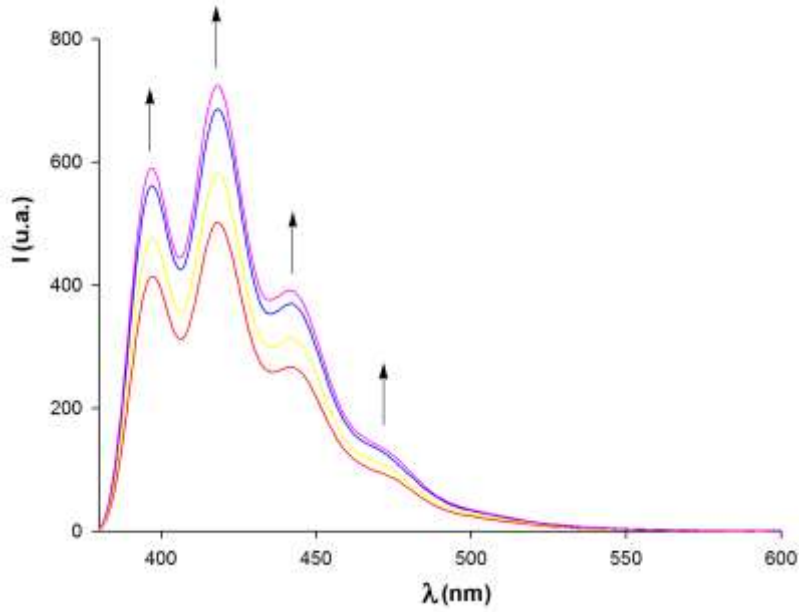

Figure S1. Changes in the fluorescence spectra of receptor $\mathbf{5^{2+}\cdot 2PF_6^-}$ (c = $1\cdot10^{-5}$ M in CH_3CN) upon addition of F^- anions from 0 to 1.8 equiv at 20 °C.

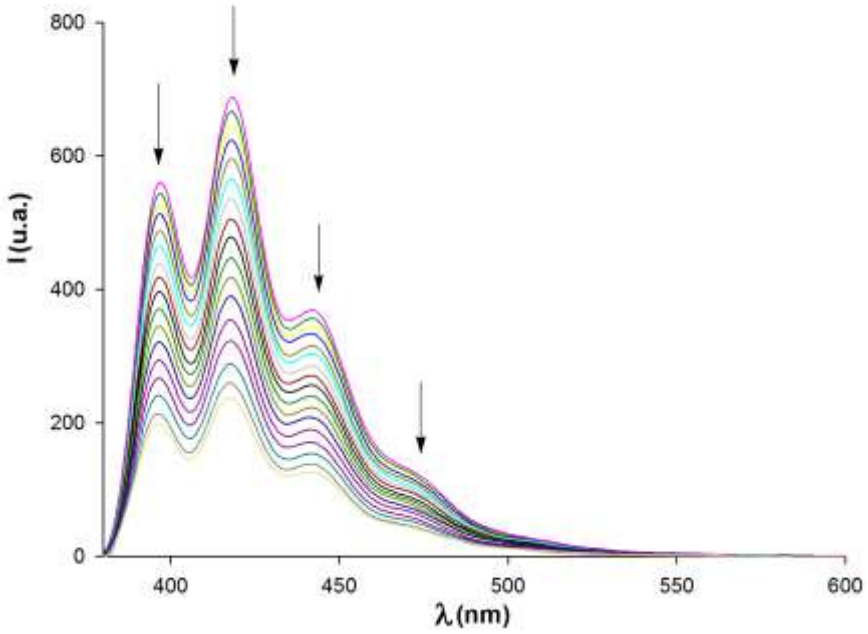

Figure S2. Changes in the fluorescence spectra of receptor $\mathbf{5^{2+}\cdot 2PF_6^-}$ (c = $1\cdot10^{-6}$ M in CH_3CN) upon addition of F^- anions from 1.8 to 5 equiv at 20 °C.

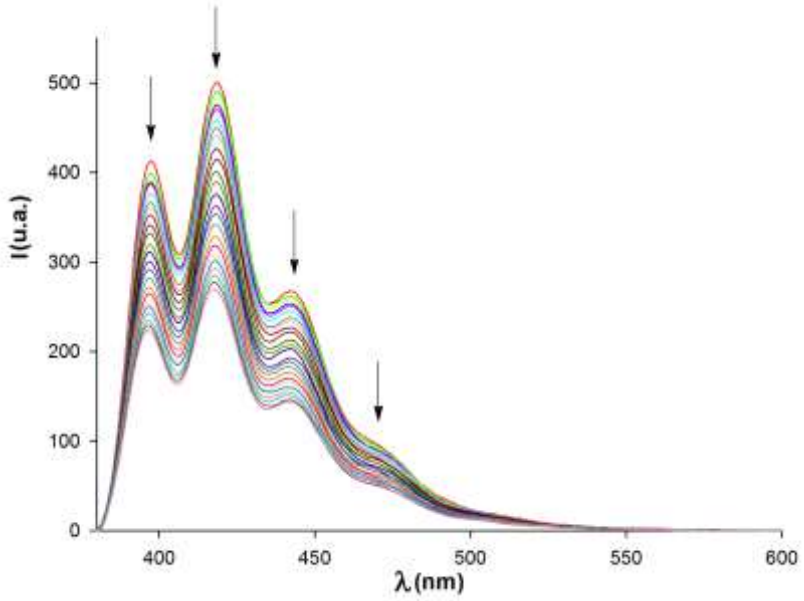

Figure S3. Changes in the fluorescence spectra of receptor $\mathbf{5^{2+}\cdot 2PF_6^-}$ (c = $1\cdot10^{-6}$ M in CH_3CN) upon addition of AcO^- anions at 20 °C.

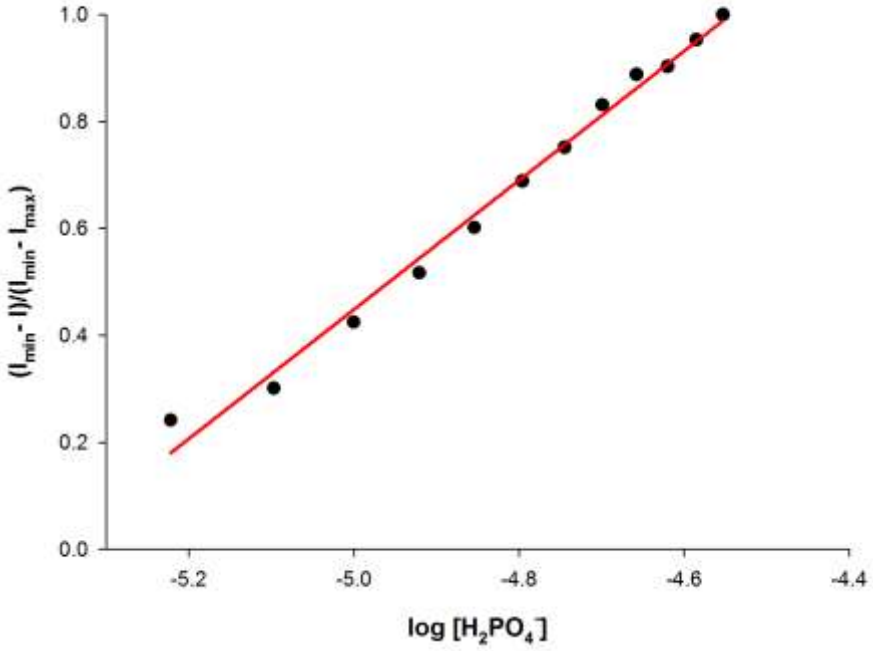

Figure S4. Fluorescence intensity of $\mathbf{5^{2+}\cdot 2PF_6^-}$ (in CH_3CN) at each concentration of $H_2PO_4^-$ added, normalized between the minimum fluorescence intensity, found at zero equiv of $H_2PO_4^-$; and the maximum fluorescence intensity. The detection limit was found at $[H_2PO_4^-] = 3.90 \times 10^{-6}$M.

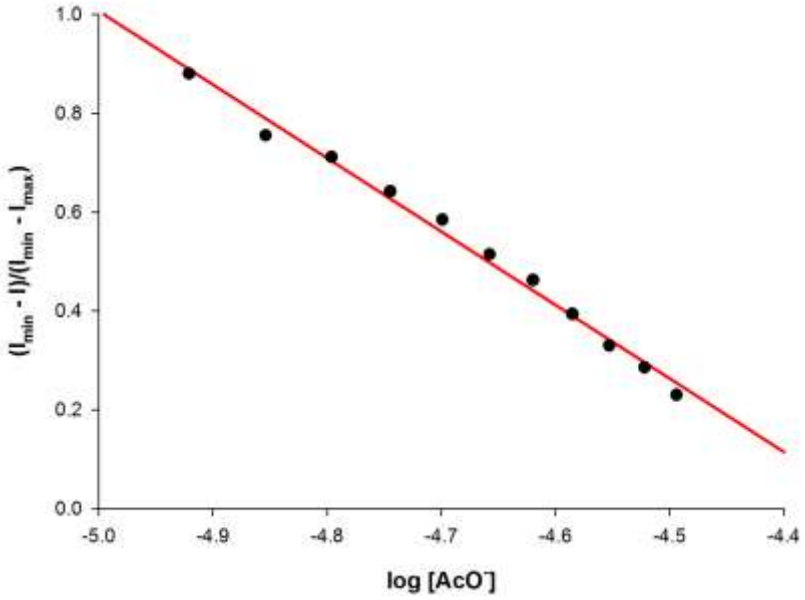

Figure S5. Fluorescence intensity of $\mathbf{5^{2+}{\cdot}2PF_6^-}$ (in CH_3CN) at each concentration of AcO^- added, normalized between the minimum fluorescence intensity, found at zero equiv of AcO^-; and the maximum fluorescence intensity. The detection limit was found at $[AcO^-]= 4.59 \times 10^{-5}$M.

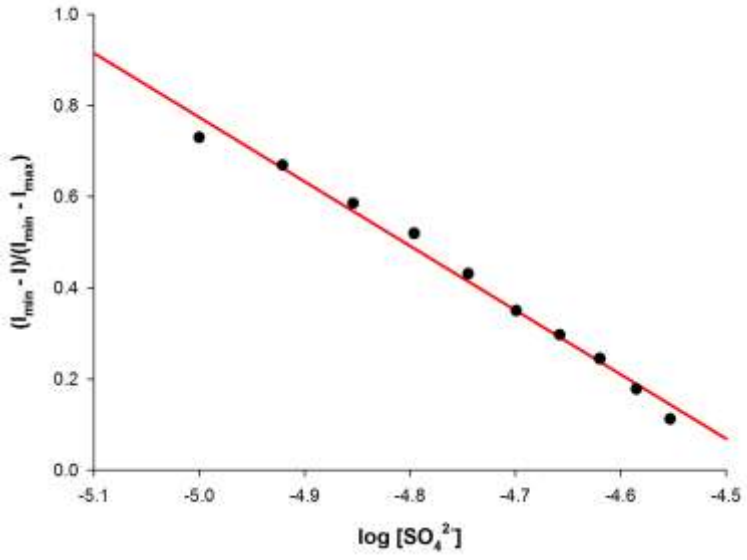

Figure S6. Fluorescence intensity of $\mathbf{5^{2+}{\cdot}2PF_6^-}$ (in CH_3CN) at each concentration of SO_4^{2-} added, normalized between the minimum fluorescence intensity, found at zero equiv of Pb^{2+}; and the maximum fluorescence intensity. The detection limit was found at $[SO_4^{2-}]= 3.57 \times 10^{-5}$ M.

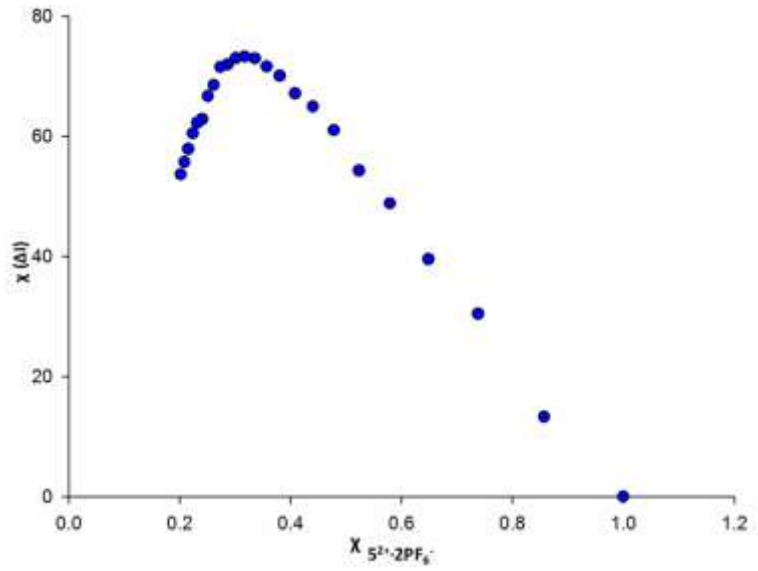

Figure S7. Job plot experiment, using the emission titration data, with a maximum at 0.33 indicating 1:2 stoichiometry for receptor $\mathbf{5^{2+}\cdot 2PF_6^-}$ and $H_2PO_4^-$ anions.

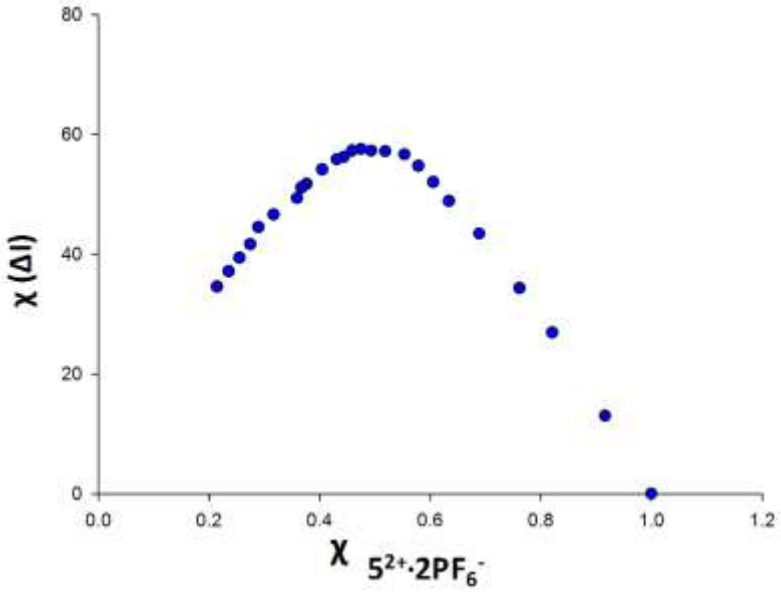

Figure S8. Job plot experiment, using the emission titration data, with a maximum at 0.5 indicating 1:1 stoichiometry for receptor $\mathbf{5^{2+}\cdot 2PF_6^-}$ and SO_4^{2-} anions.

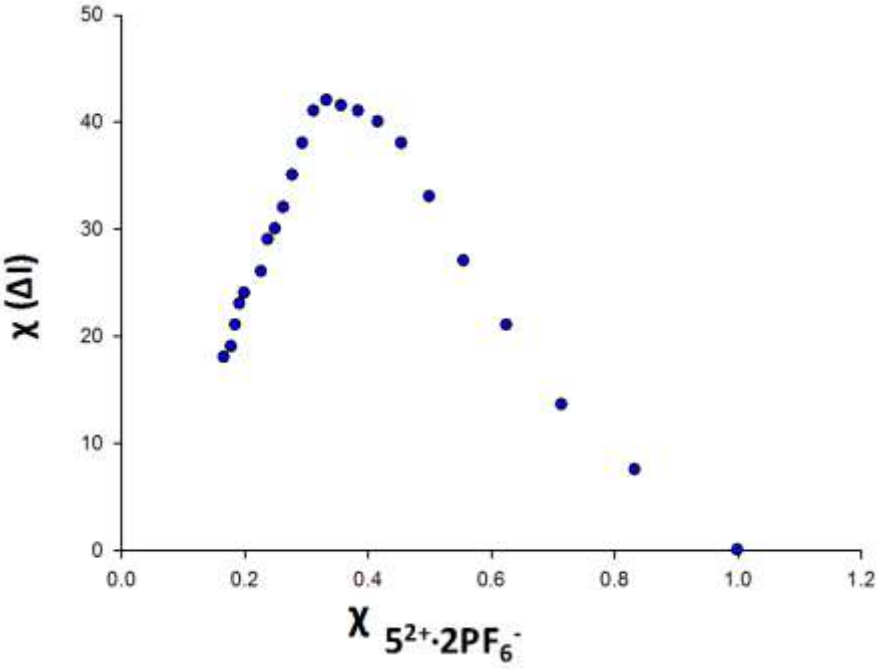

Figure S9. Job plot experiment, using the emission titration data, with a maximum at 0.33 indicating 1:2 stoichiometry for receptor $\mathbf{5^{2+}\cdot 2PF_6^-}$ and AcO^- anions.

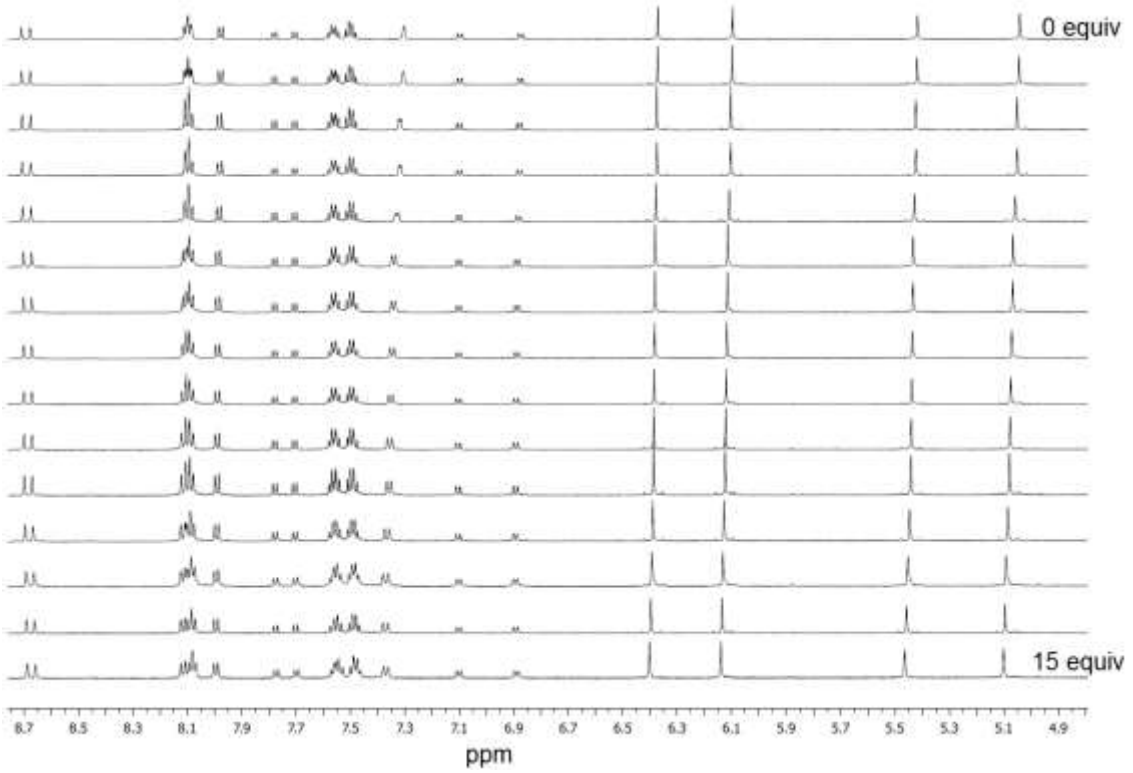

Figure S10. ^1H NMR spectral changes observed in the receptor $\mathbf{5^{2+}\cdot 2PF_6^-}$ in CD_3CN/CD_3OD (8:2, v/v) during the addition of up to 15 equivalents of SO_4^{2-} ions.

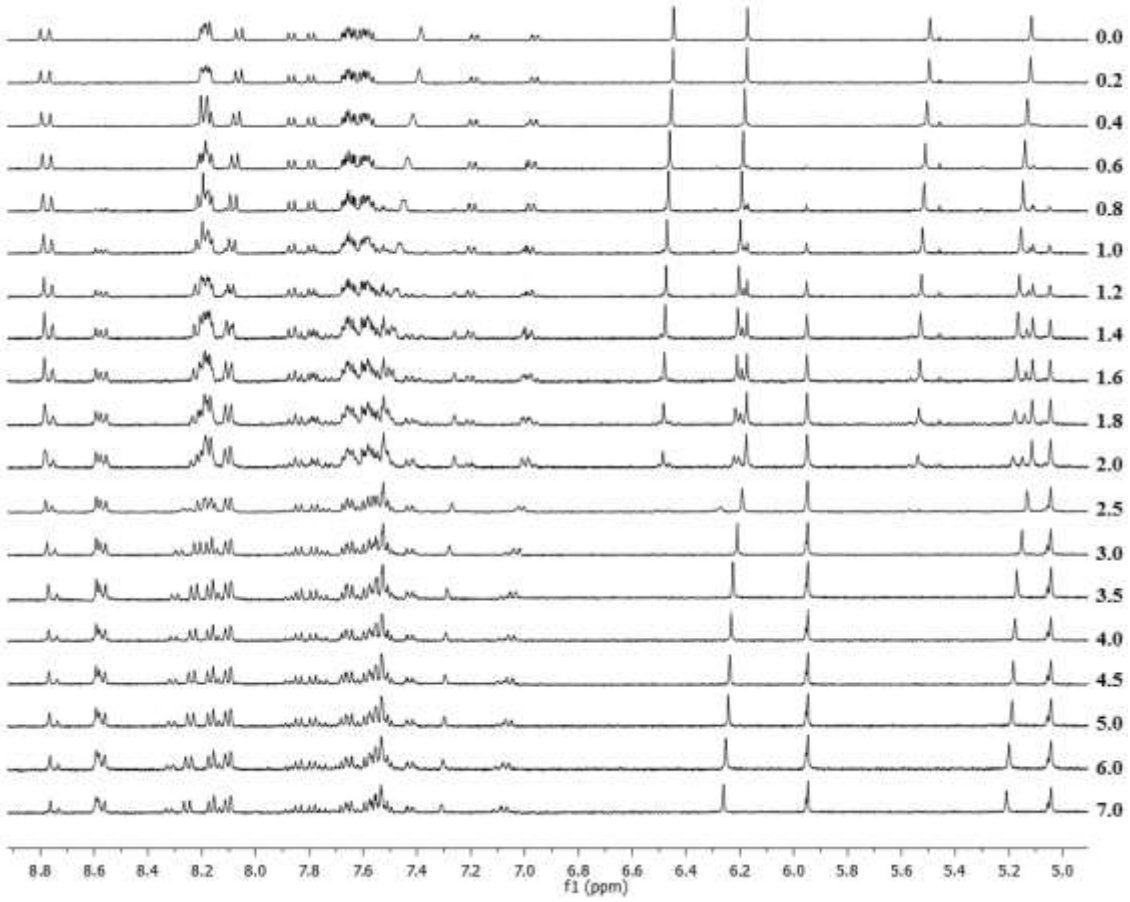

Figure S11. ^{1}H NMR spectral changes observed in the receptor $\mathbf{5^{2+}\cdot 2PF_6^-}$ in CD_3CN/CD_3OD (8:2, v/v) during the addition of up to 15 equivalents of $HP_2O_7^{3-}$ ions.

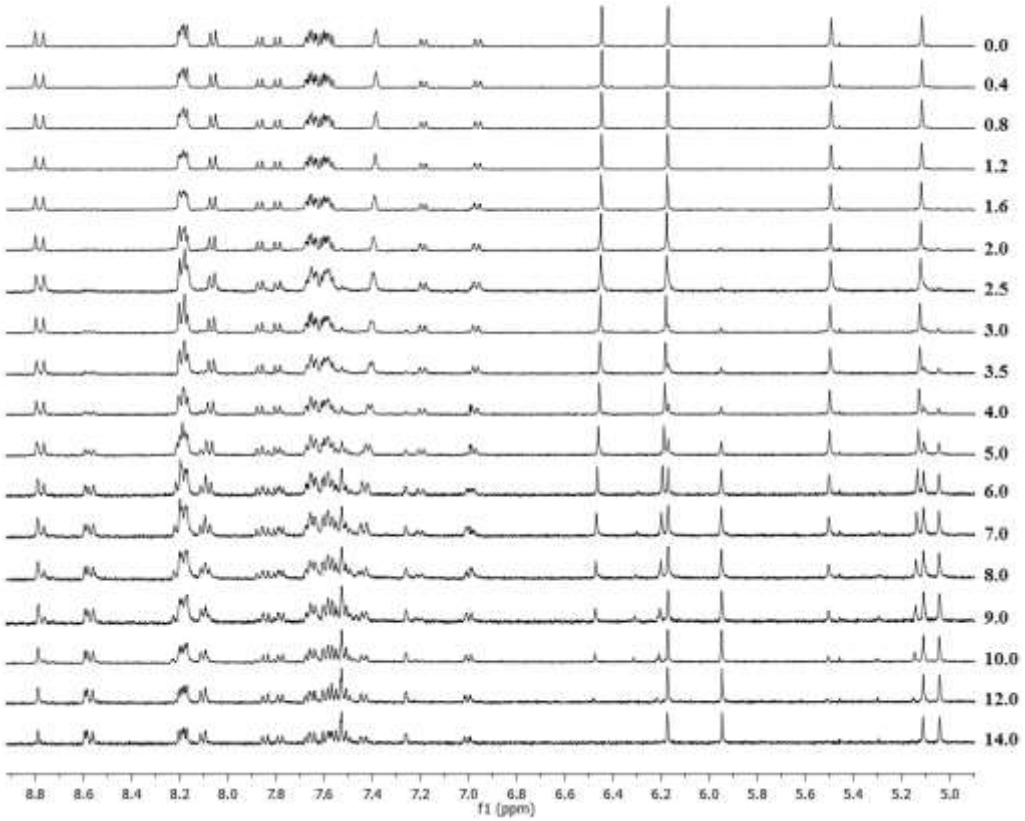

Figure S12. ^{1}H NMR spectral changes observed in the receptor $\mathbf{5^{2+}\cdot 2PF_6^-}$ in CD_3CN/CD_3OD (8:2, v/v) during the addition of up to 15 equivalents of F^- ions.

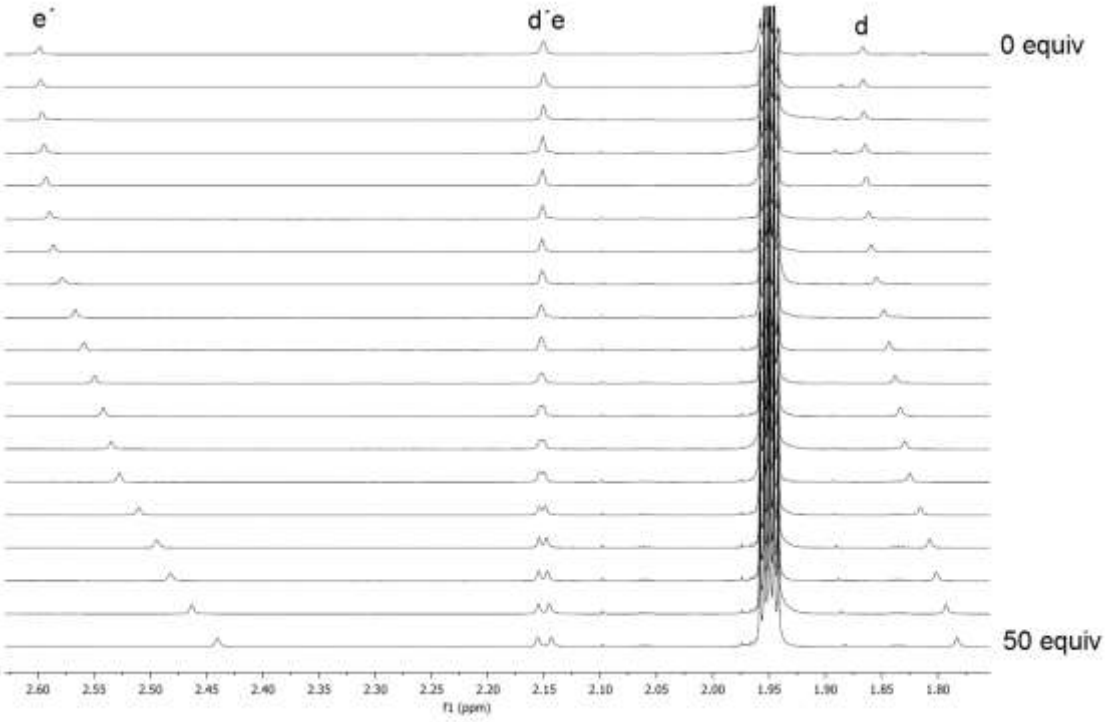

Figure S13. ^{1}H NMR spectral changes observed in the methyl protons of the receptor $\mathbf{5^{2+}\cdot 2PF_6^-}$ in CD_3CN/CD_3OD (8:2, v/v) during the addition of up to 50 equivalents of $H_2PO_4^-$ ions.

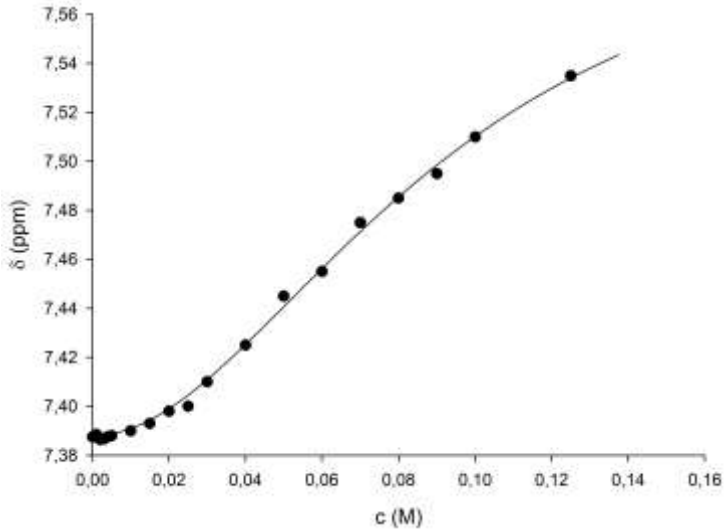

Figure S14. Changes in ^{1}H NMR spectra in the H_a proton of the receptor $\mathbf{5^{2+}\cdot 2PF_6^-}$ upon addition of increasing amounts of $H_2PO_4^-$ anions. Points represent experimental data, continuous lines represent calculate curve.

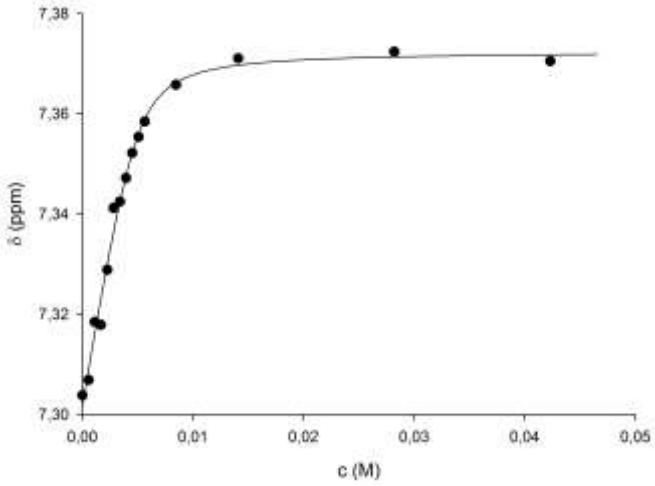

Figure S15. Changes in ^{1}H NMR spectra in the H_a proton of the receptor $\mathbf{5^{2+}\cdot 2PF_6^-}$ upon addition of increasing amounts of SO_4^{2-} anions. Points represent experimental data, continuous lines represent calculate curve.

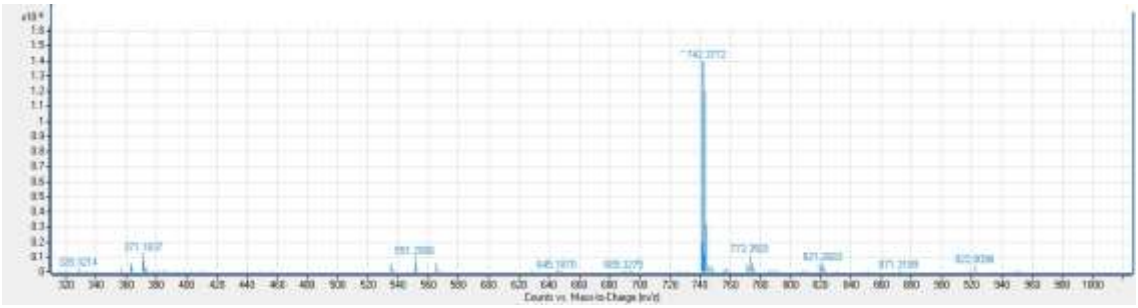

Figure S16. Mass spectrum of the solution of $\mathbf{5^{2+}\cdot 2PF_6^-}$ in CH_3CN after the addition of 3 equivalent of $HP_2O_7^{3-}$ ions, indicating the formation of the imidazolone $\mathbf{6^+\cdot PF_6^-}$ $C_{52}H_{45}N_4O^+$ (M^+ = 741.36)